7-Methylguanine: Protonation, formation of linkage isomers with *trans*-$(NH_3)_2Pt^{II}$, and base pairing properties.

Agnes Kozma, Susana Ibáñez, Radu Silaghi-Dumitrescu, Pablo J. Sanz Miguel, Deepali Gupta and Bernhard Lippert

Electronic Supplementary Material

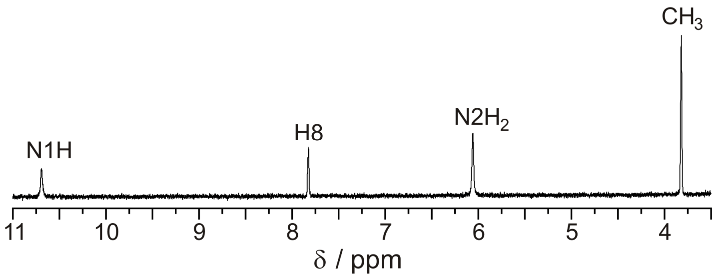

Figure S1. ^{1}H NMR spectrum (400 MHz) of a saturated solution of 7-MeGH (**1**) in wet Me_2SO-d_6 (c ≃ 0.005 M). Dilution does not cause any upfield shifts of N1H and $N2H_2$ resonances, thus ruling out any measurable self-association.

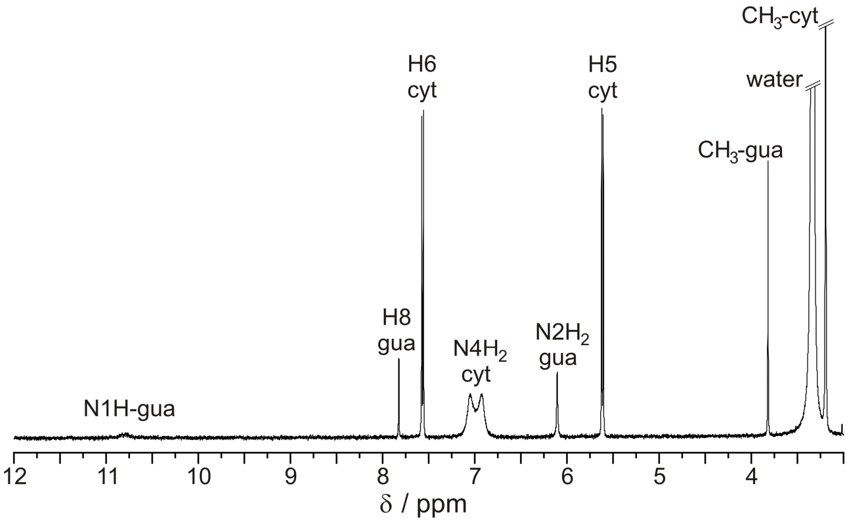

Figure S2. ^{1}H NMR spectrum (400 MHz, wet Me$_2$SO-d_6) of 7-MeGH (**1**) (c ≃ 0.0017 M) and 1-MeC (c ≃ 0.01 M). Interaction shifts $\Delta\delta$ are: N1H (**1**), 0.09 ppm, N2H$_2$ (**1**), 0.05 ppm, and N4H$_2$ (1-MeC), 0.03 ppm. Because of the large excess of 1-MeC over 7-MeGH and of signal averaging, the interaction shift of N4H$_2$ (1-MeC) is smaller than that of N2H$_2$ (**1**).

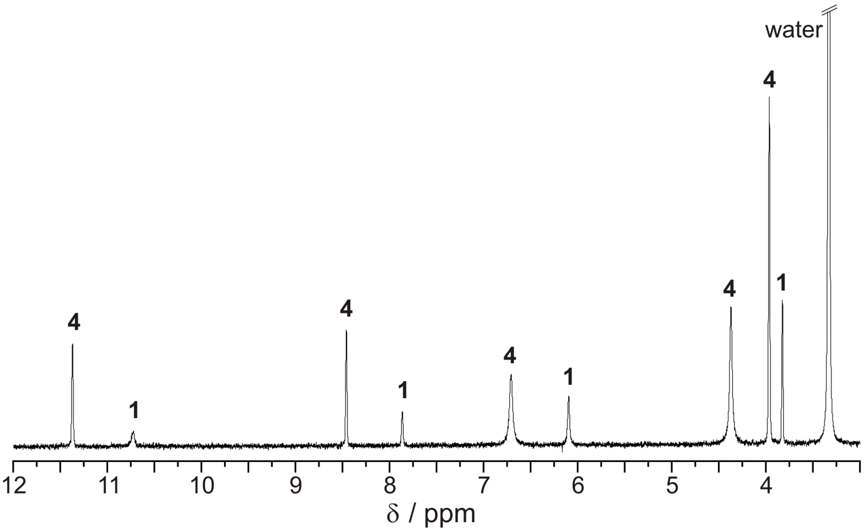

Figure S3. ^{1}H NMR spectrum of a mixture of **4** (c ≃ 0.0015 M) and 7-MeGH (**1**) (c ≃ 0.001 M) in wet Me$_2$SO-d_6.

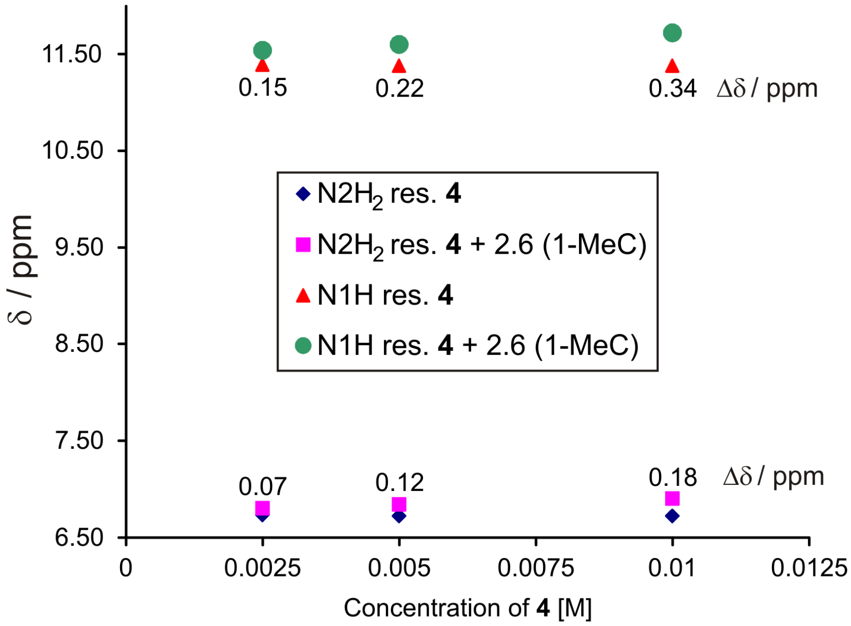

Figure S4. ^{1}H NMR interaction shifts of mixtures of **4** and 1-MeC in Me$_2$SO-d_6.

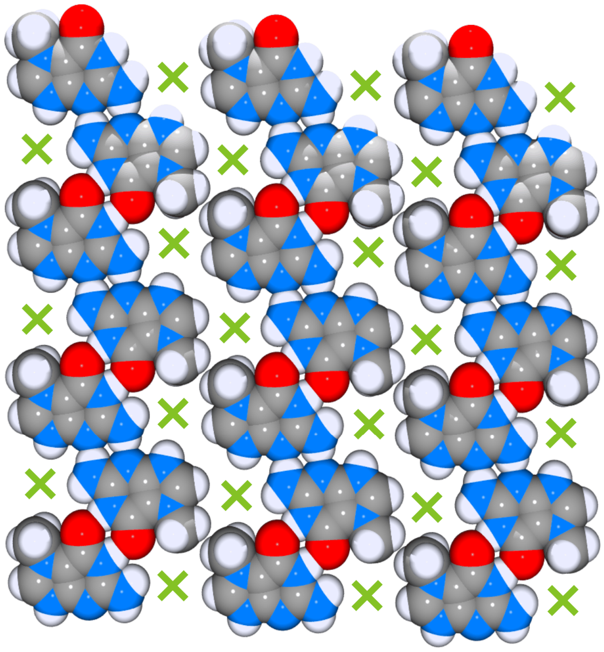

Figure S5. Space filling representation of a layer in the structures of **1**, with × showing the mutual position of counter anions.

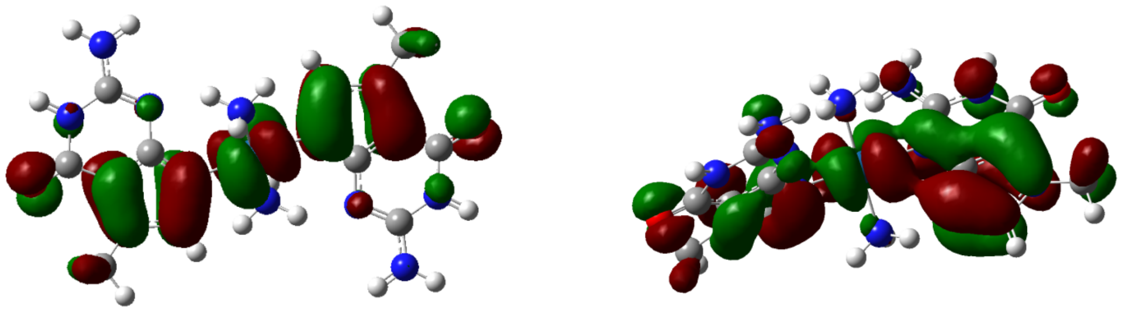

4 - HOMO -4 orbital

5 - HOMO -5 orbital

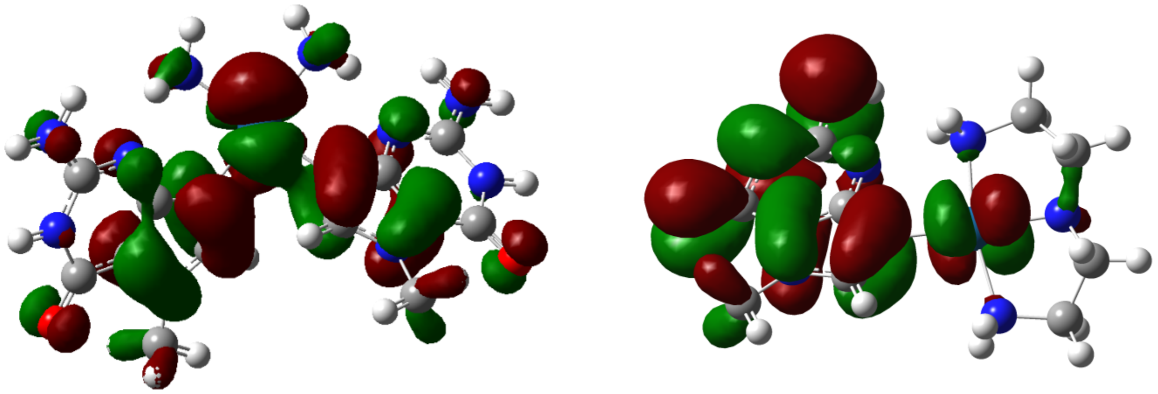

7 - HOMO -6 orbital

8 - HOMO -2 orbital

Figure S6. Molecular orbitals of compounds **4**, **5**, **7**, and **8**. The atom numbering schemes of compound **4, 5** and **8** are as used throughout the text. Tables S2 – S5 and Figure S7 summarize the experimental and theoretical data for compounds **4**, **5**, **7**, **8**, and **8a**. The dihedral angle is considered in every case between the Pt^{II} coordination plane and the 7-MeGH nucleobase. The N3···NH_3 hydrogen bond is measured between both N atoms. In the deprotonated forms, the structural features, which depend on the nucleobase, are discussed separately in the deprotonated and neutral 7-MeGH. In the case of compound **5** the two nucleobases, linked via N3 and N9 to the metal centre, are discussed separately.

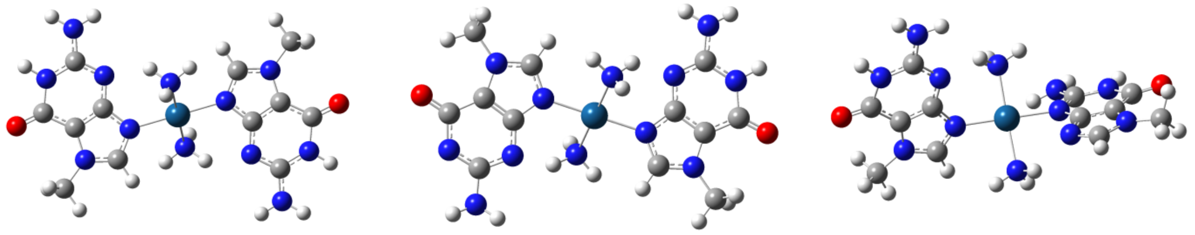

4 - neutral

4 - monodeprotonated

5 - neutral

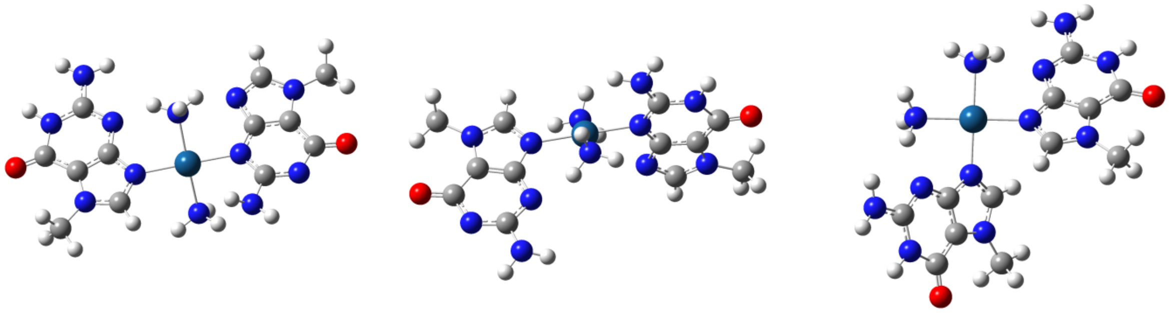

5 - monodeprotonated at N3-coordinated 7-MeGH

5 - monodeprotonated at N9-coordinated 7-MeGH

7 - neutral

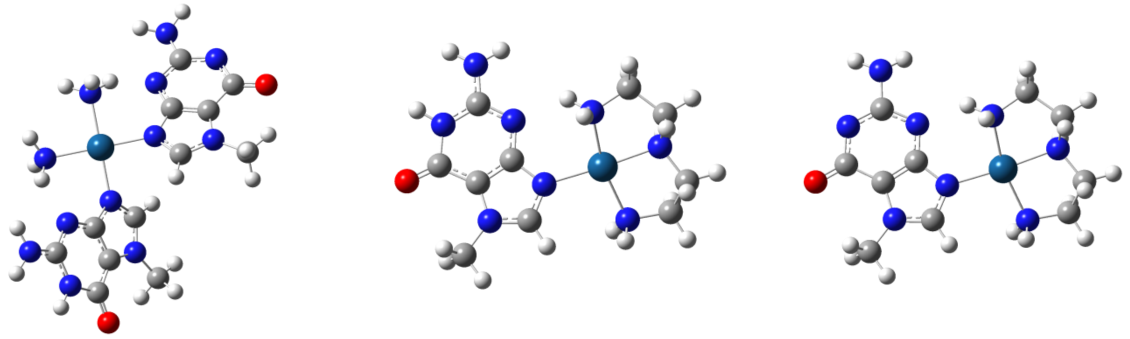

7 - monodeprotonated

8 - neutral

8 - monodeprotonated

Figure S7. Optimized structures for compounds **4**, **5**, **7**, and **8** in water. For compound **4**, the DFT-computed structure is in good general agreement with experiment, cf. Table S2. The Pt-N distances are slightly overestimated by DFT, by ca. 0.05 Å. Importantly, theory reproduces well the dihedral angles and the N9-Pt-N9 and N11-Pt-N12 angles.

Table S1. Chemical Shifts (*δ*, ppm) of ^{1}H NMR resonances of mixtures of **4** and **1** in Me_2SO-d_6.[a]

resonance	0.0015 M (**4**) 0.0010 M (**1**)	0.00075 M (**4**) 0.00050 M (**1**)	0.00038 M (**4**) 0.00025 M (**1**)	0.00019 M (**4**) 0.00130 M (**1**)
N1H (**4**)	11.37	11.38	11.39	11.38
N1H (**1**)	10.72	10.71	10.69	10.68
H8 (**4**)	8.46	8.46	8.46	8.46
H8 (**1**)	7.87	7.84	7.83	7.83
NH_2 (**4**)	6.71	6.74	6.74	6.75
NH_2 (**1**)	6.10	6.07	6.05	6.05
NH_3 (**4**)	4.37	4.37	4.37	4.37
CH_3 (**4**)	3.96	3.96	3.96	3.97
CH_3 (**1**)	3.82	3.82	3.82	3.82

[a] water content of Me_2SO-d_6: 12 H_2O molecules per **4** at highest concentration; 106 H_2O per **4** at lowest concentration.

Table S2. Selected bond lengths (Å) and angles (º) in the experimental and theoretical structures of compound **4**.

Compound/bonds and angles	Pt-N9	Pt-N9	Pt-N11	Pt-N11	Dihedral angle		N9-Pt-N9	N11-Pt-N11	$N3\cdots NH_3$	
4 experiment	2.01	2.01	2.03	2.03	47	47	180	180	2.96	2.96
4 gas phase, neutral	2.06	2.06	2.09	2.09	45	45	180	180	2.93	2.93
4 water, neutral	2.06	2.06	2.09	2.09	47	47	180	180	2.99	2.99
4 gas phase, deprot.			2.08	2.10			179	178		
deprot. nucleobase	2.03				38				2.69	
neutral nucleobase	2.08				45				2.99	
4 water, deprot.			2.09	2.09			180	180		
deprot. nucleobase	2.05				41				2.88	
neutral nucleobase	2.06				49				3.02	

Table S2 shows that, as expected, the nucleobase with –1 charge gets closer to the Pt^{II} centre (2.03 Å, 2.05 Å, vs. the 2.06 and 2.08 Å distances computed for the Pt-N bonds with the neutral nucleobases). The $N3\cdots NH_3$ hydrogen bond shortens upon deprotonation of the nucleobase (the difference in hydrogen bonds between the deprotonated and the neutral nucleobase is 0.30 Å in vacuum and 0.14 Å in water).

In the crystal structure of **5**, Pt-N3 distance is longer than Pt-N9 by ca. 0.04 Å. This difference is well reproduced by calculations. In general, as already seen for compound **4**, Pt-N distances are overestimated by DFT by ca. 0.06 Å. Theoretical dihedral angles are significantly smaller than the experimental ones; the values are decreased approximately to the half. The computed N9-Pt-N3 and N11-Pt-N12 angles are in good agreement with experiment. The $N3\cdots NH_3$ hydrogen bond appears shorter (stronger) by ca. 0.60 Å in the computed structures than in the experiment, which may be correlated with the significant changes in the dihedral angles.

Table S3. Selected bond lengths (Å) and angles (º) in the experimental and theoretical structures of compound **5**.

Compound/bonds and angles	Pt-N9 or Pt-N3	Pt-N11	Pt-N12	Dihedral angle	N9-Pt-N3	N11-Pt-N12	N3··· NH_3
5 experiment		2.03	2.05		176	177	
N3 coord. ligand	2.04			86			
N9 coord. ligand	2.00			83			3.58
5 gas phase, neutral		2.09	2.09		179	174	
N3coord. ligand	2.10			47			
N9coord. ligand	2.06			42			2.91
5 water, neutral		2.09	2.09		180	175	
N3 coord. nucleobase	2.08			56			
N9 coord. nucleobase	2.06			42			2.95
5 gas phase, deprot. at N3 coord. ligand		2.08	2.10		179	174	
deprot. nucleobase (N3)	2.06			39			
neutral nucleobase (N9)	2.09			41			3.03
5 gas phase, deprot. at N9 coord. ligand		2.08	2.10		179	173	
deprot. nucleobase (N9)	2.03			34			2.67
neutral nucleobase (N3)	2.12			47			
5 water, deprot. at N3 coord. ligand		2.08	2.10		178	175	
deprot. nucleobase (N3)	2.07			46			
neutral nucleobase (N9)	2.07			44			3.05
5 water, deprot. at N9 coord. ligand		2.09	2.09		180	175	
deprot nucleobase (N9)	2.04			39			2.87
neutral nucleobase (N3)	2.09			54			

The slight overestimation of Pt-N bond lengths is also noted for **7**, cf. Table S4. The dihedral angles are decreased compared to experiment; this is most likely due to the fact that hydrogen bonds not present in the experiment are established in the computed structure between the N3 and ammonia (N3···NH_3 distances shorter by ca. 1 Å).

Table S4. Selected bond lengths (Å) and angles (º) in the experimental and theoretical structures of compound **7**.

Compound/bonds and angles	Pt-N9	Pt-N9	Pt-N11	Pt-N12	Dihedral angle		N9-Pt-N9	N11-Pt-N12	N3···NH_3	
7 experiment	2.02	2.02	2.04	2.05	79	51	89	90	3.82	3.12
7 gas phase, neutral	2.06	2.06	2.10	2.10	39	39	92	93	2.89	2.89
7 water, neutral	2.06	2.06	2.09	2.09	40	40	91	91	2.94	2.94
7 gas phase, deprot.			2.12	2.09			91	93		
deprot. nucleobase	2.03				35				2.69	
neutral nucleobase	2.07				36				2.94	
7 water, deprot.			2.09	2.10			91	91		
deprot. nucleobase	2.06				36				2.85	
neutral nucleobase	2.07				41				2.96	

In compound **8**, Pt-N distances are again slightly overestimated by calculation (by 0.04–0.07 Å). The dihedral angles are approximately doubled compared to the experiment, which involves longer N3···NH_2 distances. There are two possible explanations for this difference. One is that stacking interactions noted in the crystal structure are not included in the DFT model, and that they are responsible for the smaller dihedral angle. The second explanation is that the DFT method overestimates here the sterical repulsion between the dien and the nucleobase hydrogen atoms.

Table S5. Selected bond lengths (Å) and angles (º) in the experimental and theoretical structures of compound **8**.

Compound/bonds and angles	Pt-N9	Pt-N1d	Pt-N2d	Pt-N3d	Dihedral angle	N3···NH_2
8 experiment	2.03	2.04	2.00	2.05	14	2.87
8 gas phase, neutral	2.06	2.08	2.07	2.12	37	2.90
8 water, neutral	2.07	2.08	2.06	2.11	37	2.95
8 gas phase, deprot.	2.03	2.06	2.08	2.14	31	2.62
8 water, deoprot.	2.06	2.08	2.06	2.11	35	2.86

As structures of compound **8a** were obtained via single point energy calculations from **8**, after adjusting the dihedral angle to 90º, the listed bond lengths in **8** do not differ from those of **8a**. Only the N3···NH_2 distances for **8a** are larger for the neutral ligand than for the deprotonated one (ca. 4 Å).